

INTERGALACTIC He II ABSORPTION IN THE SPECTRA OF QUASARS AT REDSHIFTS 3.5 AND 3.8, OBSERVED WITH THE *HST* ACS PRISM¹

WEI ZHENG,² AVERY MEIKSIN,³ KEITH PIFKO,² SCOTT F. ANDERSON,⁴ CRAIG J. HOGAN,⁴ ERIC TITILEY,³ GERARD A. KRISS,⁵
 KUENLEY CHIU,⁶ DONALD P. SCHNEIDER,⁷ DONALD G. YORK,⁸ AND DAVID H. WEINBERG⁹

Received 2008 March 28; accepted 2008 May 18

ABSTRACT

We present the UV spectra of two quasars obtained with the *Hubble Space Telescope* Advanced Camera for Surveys (*HST* ACS) prism ($R \sim 100$). One quasar, at redshift $z = 3.5$, shows an absorption edge consistent either with nearly fully ionized helium with an intergalactic He II Ly α optical depth at 304 \AA of $\tau_{304} > 3.1$ (90% confidence), or a He III region with edge 5.4 Mpc from the QSO. The spectrum of the second quasar, at $z = 3.8$, has a broad absorption profile extending across the He II emission line of the quasar consistent with a damped absorption profile from an intervening He II system at $z \simeq 3.7$ with a column density of approximately 10^{22} cm^{-2} . In this case, the extremely high He II column density and absence of strong H I absorption suggests that the radiation field is quite weak at 4 ryd. The combined He II and H I signatures are consistent with photoionization by a compact (1–100 pc) star-forming region located approximately 10 Mpc from the quasar.

Subject headings: dark matter — intergalactic medium — quasars: individual (SDSS J1711+6052, SDSS J2346-0016) — surveys — ultraviolet: general

1. INTRODUCTION

The intergalactic medium (IGM) is the largest reservoir of baryonic matter in the universe, and its complex structure has been well studied via Ly α forest lines in the spectra of bright quasars. The IGM is highly ionized, as evidenced by the lack of a Gunn-Peterson effect (Gunn & Peterson 1965) in the spectra of quasars at $z < 5.5$, as well as limited He II Ly α opacity at wavelengths blueward of $304(1+z) \text{ \AA}$ at $z \sim 2.7$ (Davidsen et al. 1996; Reimers et al. 1997; Anderson et al. 1999). The Gunn-Peterson effect of intergalactic hydrogen and helium is a powerful tool for revealing the history of IGM reionization. Since intergalactic helium is more difficult to ionize and recombines more rapidly than its hydrogen counterpart, the reionization of (singly ionized) intergalactic helium should take place later than that of hydrogen. He II absorption is therefore an important probe of the evolution of the IGM. Since its first detection at $z = 3.3$ (Jakobsen et al. 1994), such a feature has been progressively found in quasar spectra at higher redshifts: $z = 3.5$ (Zheng et al. 2004a) and $z = 3.8$ (Zheng et al. 2005). Measurements of the intergalactic helium and hydrogen Ly α opacities show He II was ionized to He III before $z \simeq 2.8$ (Reimers et al. 1997; Kriss et al. 2001), while

intergalactic hydrogen was ionized before $z \simeq 6$ (Fan et al. 2002). Theoretical models (Haardt & Madau 1996; Madau et al. 1999; Barkana & Loeb 2002; Wyithe & Loeb 2003; Cen 2003) suggest that the reionization of the IGM proceeds in several stages, evolving from cosmic “bubbles” in the vicinity of local ionizing sources that eventually fill all of intergalactic space. As the reionization of the IGM is a gradual process, it is yet unclear when it started from a virtually neutral state. Indirect observational evidence (Theuns et al. 2002; Zheng et al. 2004b; Reimers et al. 2005) suggests that the reionization of singly ionized helium started around $z \simeq 3.4$.

When the IGM becomes largely neutral, its optical depth should be $\simeq 10^5$ for hydrogen and $\simeq 10^3$ for helium. Such high optical depths should produce damped absorption profiles that cut into the flux of the Ly α emission line in the spectra of very distant objects (Miralda-Escudé 1998; Madau & Rees 2000). Such a signature must be distinguished from H I damped Ly α absorbers (DLA; Wolfe et al. 2005), which originate from discrete systems with neutral hydrogen column densities of 10^{20} – 10^{22} cm^{-2} . In this paper, we report a possible damped He II absorption feature at $z \simeq 3.8$. It is broader, however, than expected from the diffuse IGM. Instead it may indicate intense ionization by a young star-forming region. Alternatively, it may result from an intervening H I DLA at low redshift.

Distances quoted assume standard cosmological parameter values: $\Omega_m = 0.3$, $\Omega_v = 0.7$, and $h = H_0/100 \text{ km s}^{-1} \text{ Mpc}^{-1} = 0.7$ (Spergel et al. 2003).

2. OBSERVATIONS AND DATA REDUCTION

We have been carrying out *HST* snapshot surveys for candidate quasars useful for measuring intergalactic He II. Our search starts from the Sloan Digital Sky Survey (SDSS) quasar catalogs (Schneider et al. 2005, 2007). Quasars between redshift 2.7 and 4.5 and brighter than *i*-band magnitude of 19.5 are selected for UV follow-ups with *HST* or compared to *GALEX* catalogs. Only a handful ($\sim 3\%$ – 5%) of them are found to have detected UV fluxes near the objects’ He II Ly α wavelength. In addition to a number

¹ Based on observations made with the NASA/ESA *Hubble Space Telescope*, obtained at the Space Telescope Science Institute, which is operated by the Association of Universities for Research in Astronomy, Inc., under NASA contract NAS 5-26555. These observations are associated with programs GO 9759, 9806 and 10231.

² Department of Physics and Astronomy, Johns Hopkins University, Baltimore, MD 21218.

³ Scottish Universities Physics Alliance (SUPA); Institute for Astronomy, University of Edinburgh, Royal Observatory, Edinburgh EH9 3HJ, United Kingdom.

⁴ Department of Astronomy, University of Washington, Seattle, WA 98195.

⁵ Space Telescope Science Institute, Baltimore, MD 21218.

⁶ Anglo-Australian Observatory, Epping, NSW 1710, Australia.

⁷ Department of Astronomy and Astrophysics, Pennsylvania State University, University Park, PA 16802.

⁸ Department of Astronomy and Astrophysics and the Enrico Fermi Institute, University of Chicago, Chicago, IL 60637.

⁹ Department of Astronomy, Ohio State University, Columbus, OH 43210.

of discoveries at $z \sim 3$, we have found three quasars at the high- z end: one at $z = 3.51$ (SDSS J2346–0016; Zheng et al. 2004a), and two at $z = 3.80$, SDSS J171134.42+605240.48 (SDSS J1711+6052) and SDSS J161426.81+485958.7 (SDSS J1614+4859). The follow-up UV spectroscopic observations of SDSS J2346–0016 and SDSS J1711+6052 were planned for STIS, but they were switched to the ACS prism because of the STIS power failure. No follow-up *HST* observations have yet been made of the second $z = 3.8$ quasar.

The prism observations of SDSS J2346–0016 were carried out in 20 orbits between 2005 September 1 and 13, with a total exposure time of ~ 44 ks. The observations of object SDSS J1711+6052 were carried out in eight orbits between 2005 May 29 and 2006 March 8, with a total exposure of 17 ks. The data in each orbit consist of three segments of exposures: A, B, and C. The exposure times for A and B were approximately 800 s, and that for segment C varied between 400 and 640 s. Between segments A and B, the spectrograph shifts by half a pixel. Three exposures of direct images were also obtained before segment A, after segment B, and after segment C. Except for three orbits in 2005 May and June, most of the direct images were taken with an exposure time of $\simeq 100$ s. For prism PR130L, the spectral resolution is $\simeq 125$ at 1370 Å and $\simeq 95$ at 1460 Å.

The prism data were processed with the standard pipeline CALACS for flat-field and dark-current corrections. We used extraction tasks in the aXe package (ver. 1.5; Walsh et al. 2006; Kümmel et al. 2008) to produce flux- and wavelength-calibrated spectra. The direct images were processed with the IRAF task *imexam* to determine the source centroids. The extraction algorithm uses these reference positions to produce spectra from two-dimensional images, and applies position-dependent wavelength calibrations. Because of limited signal-to-noise ratio in the direct images, some of these source positions may be inaccurate by up to 1–2 pixels. We therefore inspected every segment of the extracted spectra, and marked a few that were apparently poorly aligned. These spectral segments account for less than 10% of the total data. Finally, we merged the spectral segments weighted by the exposure times to generate several spectra: the full set with or without the suspected segments, and those for each of the segments. In this paper we present the results from the full merged spectra, but since the number of suspected segments is insignificant, our conclusions would not change if a few potentially poorly aligned spectra were excluded.

The prism spectrum of SDSS J2346–0016 shown in Figure 1 displays several broad features, and the precise profile of the He II feature is not certain. There appears to be no significant He II Ly α emission line from the quasar, with a continuum flux of $\simeq 5 \times 10^{-17}$ ergs s $^{-1}$ cm $^{-2}$ Å $^{-1}$. Several possible absorption features are unidentified. The absorption edge matches the instrumental resolution profile.

However, the spectrum of SDSS J1711+6052 shown in Figure 1 displays an absorption-edge feature that is considerably broader than the instrumental profile and is consistent with damped absorption, although it is unclear whether the damped absorption is due to H I at low redshift or He II at high redshift. If the continuum flux is $\simeq 4 \times 10^{-17}$ ergs s $^{-1}$ cm $^{-2}$ Å $^{-1}$, the emission feature near 1510 Å may be the red wing of a broad He II Ly α emission line. Similar broad He II Ly α emission lines, with FWHM $> 10^4$ km s $^{-1}$, are also shown in quasar HS 1700+64 ($z = 2.73$; Davidsen et al. 1996; Fechner et al. 2006) and Q0302-004 ($z = 3.29$; Jakobsen et al. 1994; Heap et al. 2000). The distortion of the emission line blueward of the peak is suggestive of strong absorption. It is shown below that it may be fit by a combined He II Ly α emission

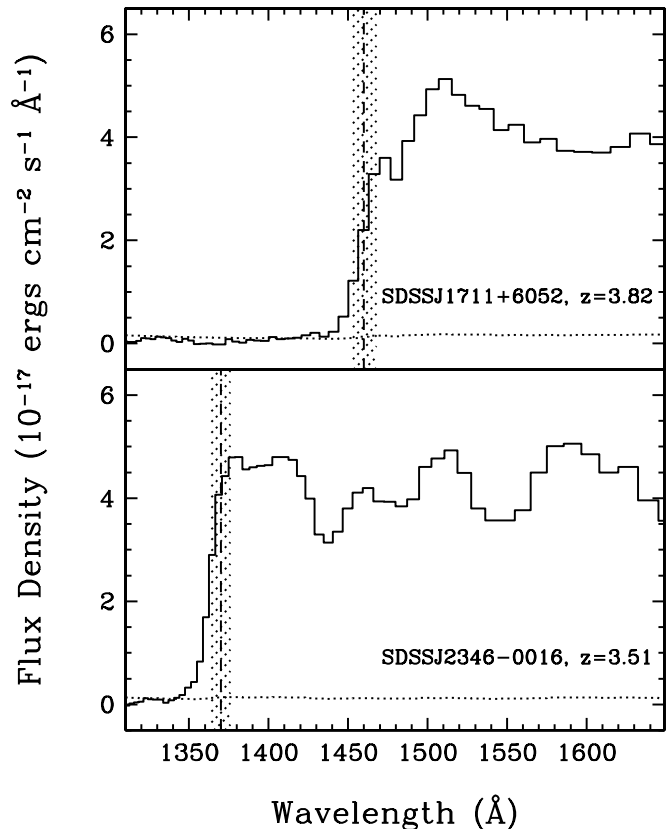


FIG. 1.—UV prism spectra of quasar SDSS J2346–0016 ($z = 3.51$) and SDSS J1711+6052 ($z = 3.80$). Propagated errors are plotted as dotted lines. The dashed lines mark the expected wavelengths of He II Ly α , and the shaded regions represent the range of the spectral resolution of the *HST* ACS prism PR130L.

line from the QSO and the red wing of an intervening damped Ly α absorber. There are two possibilities for the nature of the damped system: (1) a He II DLA at $z \simeq 3.7$, or (2) an H I DLA at $z \simeq 0.2$. We discuss each of these possibilities below.

The quasar redshifts from the SDSS (Schneider et al. 2007) are $z = 3.489$ for SDSS J2346–0016 and $z = 3.827$ for SDSS J1711+6052. These values are derived from the SDSS pipeline (Stoughton et al. 2002). We inspected the SDSS spectra and found the redshift values suited for the H I Ly α absorption edge are 3.51 and 3.80, respectively, without assuming local velocities. Given the low spectra resolution of the prism data, our results below are not affected by small differences in redshift.

3. DISCUSSION

3.1. He II Ionization Region

In the vicinity of a bright quasar, the ionization radiation field will have an increased intensity due to the radiation from the quasar. This “proximity effect” should apply to He II absorption (Zheng & Davidsen 1995; Hogan et al. 1997), as well as hydrogen absorption, for which it has been detected (Murdoch et al. 1986; Bajtlik et al. 1988). The proximity profile may be described by a position-dependent optical depth $\tau = \tau_0 / (1 + \omega)$, where τ_0 is the average IGM opacity unaffected by the quasar luminosity and ω is the ratio of quasar flux to that of intergalactic radiation. Its confirmation is difficult because it requires an unambiguous detection of the asymptotic amount of absorption distant from the QSO. If the signal is detectable only in the region for which $\omega \gg 1$, no value for τ_0 may be determined without an independent value for the UV

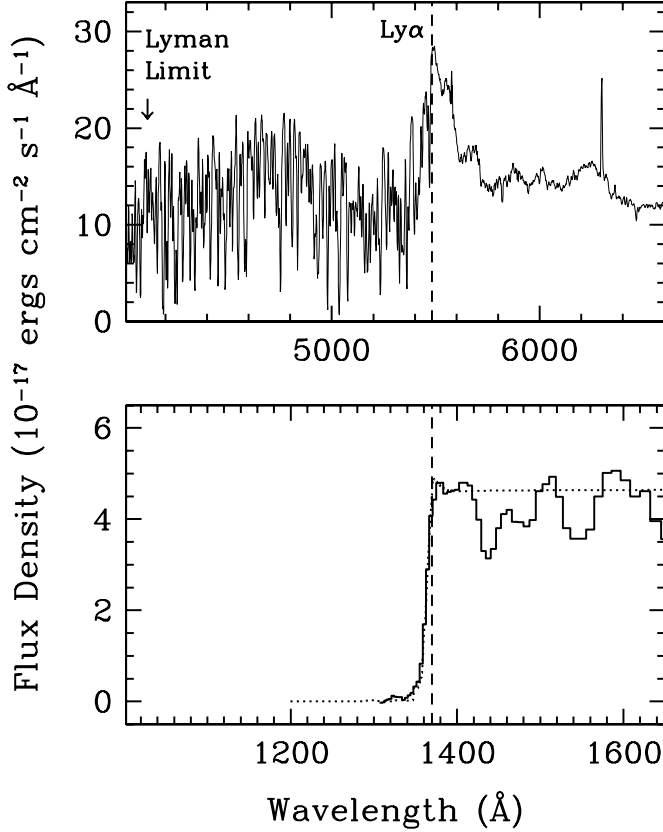


FIG. 2.—Comparison of H I (top panel) and He II (bottom panel) spectra in quasar SDSS J2346–0016. The optical spectrum (top panel) is from the SDSS, and the wavelength of the redshifted H I Lyman limit is marked with an arrow. (Strong residuals resulting from inadequate sky subtraction are present at 5585 and 6300 \AA .) The dotted line in the bottom panel shows the best-fit reionization model.

He II-ionizing background. For this reason, we instead model the absorption as He II ionization zones produced by the quasars.

We ran reionization simulations using methods similar to Tittley & Meiksin (2007) but adapted to a point radiation source. The gas density is assumed to trace the dark matter in a 256^3 N -body simulation in a box with a comoving side of length $25 h^{-1} \text{ Mpc}$. The initial density perturbations were generated from a COBE-normalized $n = 0.97$ power spectrum. Two simulations were required to generate the lines of sight, one with the source placed at the center of the volume with radiative transfer performed on a polar grid, and a second ionized by a plane wave passing across the volume to model the extended environment of the source. The source for the polar grid run is a QSO-like $L \propto \nu^{-0.5}$ power-law spectrum for $z < 4.5$. The plane-wave simulation used a $L \propto \nu^{-1}$ power-law flux designed to mimic the intergalactic radiation field. For the plane-wave simulation only, ionization to He III was prevented within the code to provide the maximal He II absorption for the data modeling and to provide the proper boundary-condition matching between the plane-wave run and the polar run, in which the He III front is just reaching the edge of the volume at $z = 3.8$.

We fit the data for SDSS J2346–0016 with a grid of model parameters, convolved with the prism instrument profile. The fit is based on lines of sight drawn through our reionization simulations. The absorption profile in Figure 1 near the quasar is accounted for primarily by the prism instrumental response function, with a smaller contribution due to the geometric $(1/r^2)$ dilution of the radiation field of the quasar. As Figure 2 shows, an excel-

lent fit is obtained, with a reduced $\chi^2 = 0.3$. The best-fit parameters, with 90% confidence intervals, are the following:

1. He III front at $z = 3.487 \pm 0.003$;
2. QSO continuum level at $(4.6 \pm 0.2) \times 10^{-17} \text{ ergs s}^{-1} \text{ cm}^{-2} \text{ \AA}^{-1}$;
3. QSO emission-line flux = $(5 \pm 5) \times 10^{-17} \text{ ergs s}^{-1} \text{ cm}^{-2}$ with FWHM = $26^{+800}_{-26} \text{ \AA}$ (observed).

For the best fit, the He III-ionizing front is 5.4 Mpc in proper distance from the quasar, displaced by the line-of-sight velocity $v \simeq -2000 \text{ km s}^{-1}$. The wavelength uncertainties in the prism data, on the order of $dz \simeq 0.03$, do not affect the size of the He III zone, as it depends only on the shape of an absorption profile. Alternatively, the helium may be ionized predominantly to He III, with a He II Ly α optical depth at 304 \AA of $\tau_{304} > 3.1$ (90% confidence) at $z \simeq 3.35$.

3.2. Damped Absorption Profile

Figure 1 shows a more complex spectrum for SDSS J1711+6052, which includes a broad He II Ly α emission line that appears to be heavily absorbed on the blue side. A He II ionization zone surrounding the quasar is not able to account for the profile, even including the full Voigt profile absorption from foreground He II assuming all of the helium is singly ionized. We attempted to reproduce the absorption with a variety of dense foreground structures from our simulations, but none came even close to creating the wide damping wing required. An acceptable fit, however, is obtained by combining the ionization from the quasar with a foreground damped Ly α absorption system. We fit the data with a power-law continuum, an emission line, and an absorption edge, convolved with the instrumental profile. The apparent absorption feature at $\lambda = 1480 \text{ \AA}$ is excluded. The best fit, shown in Figure 3, is for a continuum level of $3.9 \times 10^{-17} \text{ ergs s}^{-1} \text{ cm}^{-2} \text{ \AA}^{-1}$ with a He II Ly α emission-line flux of $4 \times 10^{-15} \text{ ergs s}^{-1} \text{ cm}^{-2}$ and FWHM of 130 \AA (observed), and a reduced χ^2 of 1.8. A slightly improved fit is found by allowing for an additional absorption feature at $\lambda = 1480 \text{ \AA}$; however, the feature is not well constrained because of the breadth of the instrumental profile and so its fitting was not further pursued. The marginalized maximum likelihood values, with 90% confidence intervals, are

1. QSO continuum = $(4 \pm 1) \times 10^{-17} \text{ ergs s}^{-1} \text{ cm}^{-2} \text{ \AA}^{-1}$;
2. QSO emission-line flux = $(6 \pm 4) \times 10^{-15} \text{ ergs s}^{-1} \text{ cm}^{-2}$ with FWHM = $120^{+190}_{-30} \text{ \AA}$.

The nature of the damped absorber, however, is unclear. It could arise from an H I DLA at $z \simeq 0.16^{+0.02}_{-0.01}$ with a column density of $4^{+16}_{-3} \times 10^{21} \text{ cm}^{-2}$ or a He II DLA at $z \simeq 3.64^{+0.07}_{-0.04}$ with a column density of $1.5^{+7.0}_{-1.0} \times 10^{22} \text{ cm}^{-2}$. We next discuss the plausibility of each of these.

An SDSS image of the quasar shows one galaxy centered within $\sim 5''$ – $6''$ of the quasar and another within about $15''$. There are no spectroscopic redshifts for these objects, but the standard SDSS photometric redshift estimates (“PhotoZ” and “PhotoZ2”) for the galaxy closer in projection range from $z = 0.24$ to 0.28 (with estimated errors of 0.03–0.08), and from $z = 0.21$ to 0.24 (with estimated errors of 0.01–0.04) for the more distantly projected galaxy. These values are consistent with the H I DLA interpretation. H I DLA systems always show low-ionization metal absorption features with velocity spreads ranging from 15 km s^{-1} to several hundred km s^{-1} (Wolfe et al. 2005). The detection of corresponding metal absorption systems would verify the H I DLA interpretation. Because O I has a nearly identical ionization potential to H I, allowing for a minimal metallicity of 0.0025 solar (Wolfe

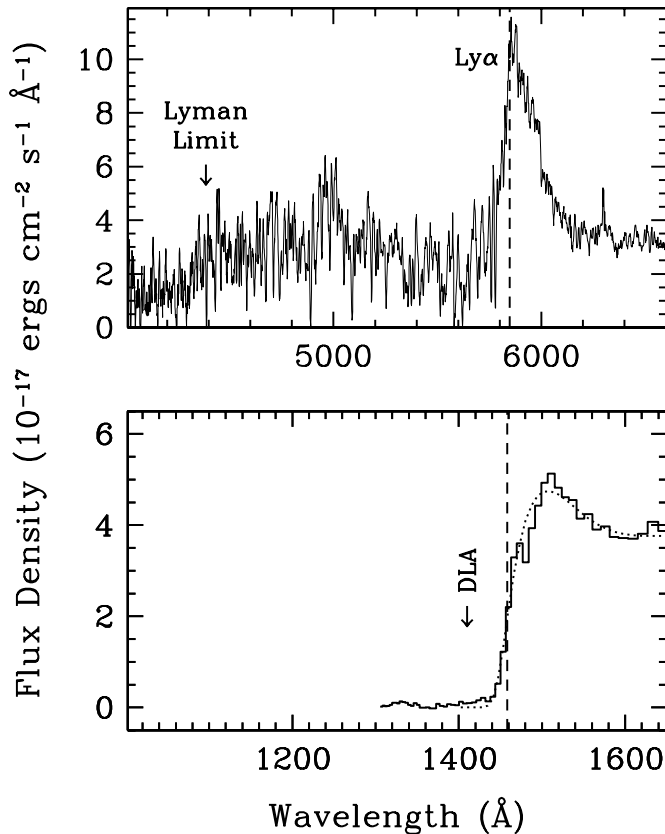


FIG. 3.—Comparison of H I and He II spectra in quasar SDSS J1711+6052. The optical spectrum (*top panel*) is from the SDSS, and the wavelength of the redshifted H I Lyman limit is marked with an arrow. In the bottom panel, the dotted line shows the best-fit absorption profile, including a damped He II Ly α absorber. The wavelength for a He II DLA is marked with an arrow.

et al. 2005) would produce a highly saturated O I λ 1302 absorption line lying in the range of observed wavelengths 1500–1540 Å. No feature is clearly visible. An equivalent width as small as 0.5 Å could be measured at the 1 σ level against the best-fitting continuum. For a saturated line of wavelength λ , the equivalent width is approximately $3(b/c)\lambda$, where b is the Doppler parameter, or the velocity spread for an absorption complex. At the 3 σ level, any saturated feature must have a velocity spread of under 95 km s $^{-1}$ to have escaped detection. Such a value lies within the range of measured velocity widths of H I DLA systems, so that the absence of the feature cannot rule out the H I DLA interpretation.

If most of the metals were doubly ionized, as is common in H I DLAs, then the Ca II λ 3935, 3970 doublet should be visible in the observed wavelength range 4520–4680 Å, and a line from Ti II λ 3385 would occur at 3890–3990 Å for a metallicity of about 0.1 solar. Other metal lines detectable in principle based on wavelength and strength, and if they form the dominant ionization species, would arise from the Na I λ 25891, 5898 doublet, Al I λ 3945, Ca I λ 4228, Ti I λ 3983, and Fe I λ 3721 and λ 3861, although these lines are seldom, if ever, found in H I DLAs. A pair of medium-resolution spectra ($R \simeq 5000$) with the 3.5 m telescope at the Apache Point Observatory (APO) does not indicate signs for any of the above absorption lines above EW of 0.3 Å.

If the feature is due to an intervening He II DLA, the best-fit places the absorber at $V = -10,300^{+4500}_{-2700}$ km s $^{-1}$ from the quasar along its line of sight, corresponding to a proper distance of 25^{+11}_{-7} Mpc (90% confidence level). Adopting a total helium column density for the absorber of $\sim 10^{22}$ cm $^{-2}$ gives a total hydrogen column density of $\sim 10^{23}$ cm $^{-2}$. This is significantly higher

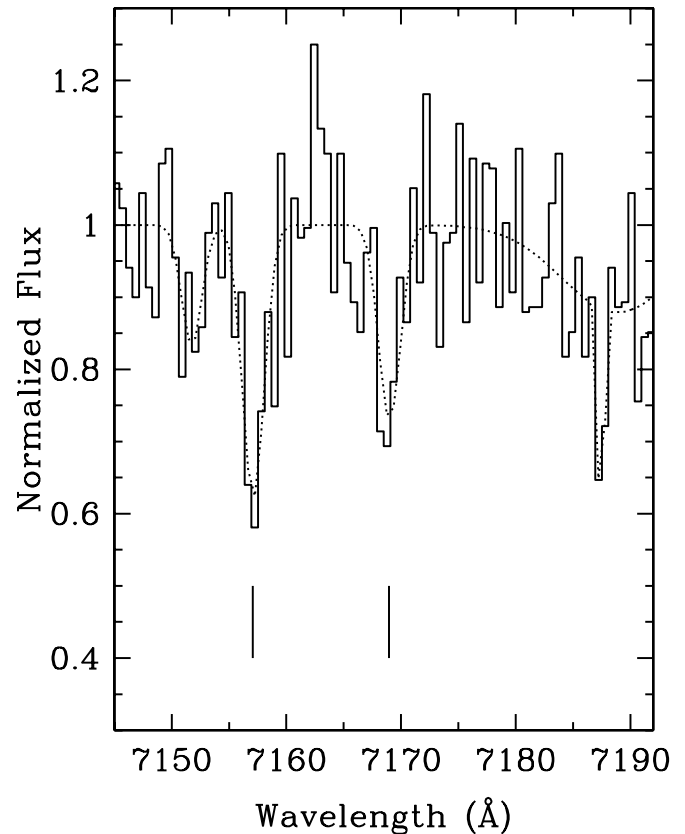


FIG. 4.—Fit to C IV absorption feature. The spectrum was obtained with 4 hr of exposure at the APO. The spectral resolution is $R \simeq 6000$, and the signal-to-noise ratio is ~ 12 pixel $^{-1}$ of width 0.58 Å. The significance for each of the C IV components is $>4 \sigma$, while other potential narrow absorption features in this wavelength region are at $<2 \sigma$ significance.

than the highest H I DLA measured (Wolfe et al. 2005). Figure 3 displays the optical spectrum of the SDSS J1711+6052, from the SDSS database and aligned to the He II counterpart. The expected corresponding H I DLA, however, is absent. Interestingly, an H I Lyman limit system is present slightly blueward of the Lyman Limit wavelength in the quasar rest frame. We find a best-fit wavelength of about 4347 ± 30 Å, corresponding to an absorption redshift $z_a = 3.77 \pm 0.03$, and an optical depth of 0.82 ± 0.13 . The redshift of this system is marginally consistent with that found for the He II DLA from the UV prism spectrum, with the absorber located approximately 6 ± 5 Mpc (proper distance) from the quasar.

If the He II absorption feature is due to a He II damped Ly α absorber, then most of the hydrogen must be ionized in the absorber. This would be the most extreme ratio of He II to H I ever detected in the IGM. We ran a suite of CLOUDY ionization models (Ferland et al. 1998) to study the ionization state of hydrogen and helium. Assuming 1000 O-stars with a surface temperature of 46,000 K in a nebula of 10^{-4} Milky Way ISM abundances (so that metal cooling is negligible) with a hydrogen density of 1.8×10^4 cm $^{-3}$ (similar densities are found in the Orion Nebula) produces an H II region with a radius of 1.0 pc, a typical He II column density through the ionized region of 8×10^{21} cm $^{-2}$, and H I column density of 10^{17} cm $^{-2}$, giving an H I Lyman Limit optical depth of 0.8. Almost all the carbon is in the form of C IV, giving a C IV column density of 10^{15} cm $^{-2}$ (for 10^{-4} Milky Way ISM abundances). For a minimal abundance of 0.0025 solar, it would produce a saturated doublet feature somewhere in the observed wavelength range 7100–7300 Å. Two absorption features

are detected in this range in the SDSS spectrum. One is at $\lambda = 7104 \text{ \AA}$ with an observed equivalent width of 1.65 \AA (4.3σ significance). Another is detected at $\lambda = 7159 \text{ \AA}$ with an observed equivalent width of 1.4 \AA (4σ significance). We identify a doublet at $7157.10/7168.98 \text{ \AA}$ in the spectrum taken with the red channel of APO's Dual Imaging Spectrograph (Fig. 4). The EW of each component is 0.89 ± 0.21 and $0.62 \pm 0.19 \text{ \AA}$, respectively. The blue component is consistent with the SDSS detected component. Although the red component is not clearly detected in the SDSS spectrum, a trough occurs coincident with the trough in the APO spectrum, which occurs at the correct wavelength separation to be identified as C iv. This suggests the presence of a C iv absorption feature at $z = 3.623$.

We also examined STARBURST99 simulations (Leitherer et al. 1999) with reference to SDSS J1711+6052. An instantaneous burst of star formation producing $10^6 M_\odot$ stars with masses $1 < M < 100 M_\odot$ following a Salpeter IMF would produce 2000–4000 O-stars lasting $(6\text{--}10) \times 10^6 \text{ yr}$, depending on metallicity. Continuous star formation at the rate $1 M_\odot \text{ yr}^{-1}$ achieves a steady population of $(20\text{--}30) \times 10^3$ O-stars after 10^7 yr . (Decreasing the upper limit to $30 M_\odot$ reduces these numbers by about 0.18 dex.)

These are moderate requirements for a small system like a globular star cluster. For larger numbers N_* of O-stars, the required total hydrogen density and size of ionized region scale like $n_H \simeq 1.8 \times 10^7 N_*^{-1} \text{ cm}^{-3}$ and $R \simeq 0.001 N_* \text{ pc}$. For $N_* = 10^5$ O stars, the required hydrogen density is $n_H = 180 \text{ cm}^{-3}$ and ionized region $R = 100 \text{ pc}$, corresponding to a continuous star formation rate of $3\text{--}4 M_\odot \text{ yr}^{-1}$. Systems with larger N_* are ruled out, as they would produce a He II Ly α flux exceeding $3 \times 10^{-18} \text{ ergs s}^{-1} \text{ cm}^{-2} \text{ \AA}^{-1}$ in the observed wavelength range $1415\text{--}1445 \text{ \AA}$, exceeding the mean measured flux in this range. (This constraint becomes less severe if dust is present, which may absorb the He II Ly α photons.)

4. CONCLUSIONS

Measurements show the intergalactic He II optical depth rises rapidly from $z = 2$ to $z = 3.5$, where it takes on a wide range of values (Zheng et al. 2004a, 2004b; Fechner et al. 2006). The rapid rise and fluctuations are suggestive of the approach to the epoch of He II reionization. We measure high He II Ly α optical depths in two QSO spectra. The optical depth in a quasar at $z \simeq 3.5$ has a lower limit of $\tau_{304} > 3.1$ (90% confidence level), while a quasar at $z \simeq 3.8$ shows a damped Ly α absorption system nearby, although it is unclear whether the damped absorption is due to H I at low redshift or He II at high redshift.

We perform reionization simulations and find an acceptable fit to the measured spectra for a He III region of radius 5.4 Mpc for

the $z = 3.5$ quasar into an IGM in which the helium is still singly ionized. No line of sight in the simulation volume is found adequate for building up the breadth of the feature in the $z = 3.8$ quasar spectrum from the radiative damping wing arising from the foreground IGM. An acceptable fit is found by introducing a damped Ly α absorption system, although the nature of the damped absorber is undetermined. It could arise either from an intervening H I absorber at $z \simeq 0.2$ with $N_{\text{H I}} \simeq 4 \times 10^{21} \text{ cm}^{-2}$ or from an intervening He II absorber at $z \simeq 3.7$ with $N_{\text{He II}} \simeq 10^{22} \text{ cm}^{-2}$, corresponding to a total hydrogen column density of $N_{\text{H,tot}} \simeq 10^{23} \text{ cm}^{-2}$.

Expected saturated metal absorption features corresponding to an H I DLA at $z \simeq 0.2$ are not found, although higher quality data are required to rule out these features at a metallicity level corresponding to the minimum established in other H I DLA systems. If the damped absorption in the $z = 3.8$ quasar spectrum arises from He II, the absence of the corresponding H I damped Ly α absorber in the SDSS spectrum requires a soft intense source of ionizing photons capable of ionizing virtually all of the hydrogen and none of the He II. The SDSS spectrum shows an H I Lyman limit system marginally consistent with the redshift of the damped He II absorber. Using photoionization models, we are able to reproduce the inferred He II and H I column densities with $10^3\text{--}10^5$ O-stars in a region $1\text{--}100 \text{ pc}$ in radius. This suggests that we may have discovered an active star-forming region, possibly as small as a globular star cluster or as large as the thickness of a dwarf galaxy. For a metallicity exceeding 10^{-5} solar, a saturated C iv absorption feature is expected. A medium-resolution APO spectrum suggests the presence of the feature, although a higher signal-to-noise ratio spectrum is needed to unambiguously confirm the detection.

Support for this research was provided by NASA through grants GO-9759, 9806 and 10231 from the Space Telescope Science Institute, which is operated by the Association of Universities for Research in Astronomy, Inc., under NASA contract NAS 5-26555. This research has made use of the aXe extraction software, produced by ST-ECF, Garching, Germany. We are extremely thankful to Dr. M. Kümmel for his invaluable help with the aXe tasks. David Syphers provided useful comments. Calculations were performed with version 07.02.01 of CLOUDY, last described by Ferland et al. (1998). The simulations were performed using a supercomputer funded by SUPA.

The optical spectra were obtained with the APO 3.5 m telescope, which is owned and operated by the Astrophysical Research Consortium.

REFERENCES

- Anderson, S. F., Hogan, C. J., Williams, B. F., & Carswell, R. F. 1999, *AJ*, 117, 56
 Bajtlik, S., Duncan, R. C., & Ostriker, J. P. 1988, *ApJ*, 327, 570
 Barkana, R., & Loeb, A. 2002, *ApJ*, 578, 1
 Cen, R. 2003, *ApJ*, 591, 12
 Davidsen, A. F., Kriss, G. A., & Zheng, W. 1996, *Nature*, 380, 47
 Fan, X., et al. 2002, *AJ*, 123, 1247
 Fechner, C., et al. 2006, *A&A*, 455, 91
 Ferland, G. J., Korista, K. T., Verner, D. A., Ferguson, J. W., Kingdon, J. B., & Verner, E. M. 1998, *PASP*, 110, 761
 Gunn, J., & Peterson, B. 1965, *ApJ*, 142, 1633
 Haardt, F., & Madau, P. 1996, *ApJ*, 461, 20
 Heap, S. R., et al. 2000, *ApJ*, 534, 69
 Hogan, C. J., Anderson, S. F., & Rugers, M. H. 1997, *AJ*, 113, 1495
 Jakobsen, P., et al. 1994, *Nature*, 370, 35
 Kriss, G. A., et al. 2001, *Science*, 293, 1112
 Kümmel, M., Walsh, J. R., Pirzkal, N., Kuntschner, H., & Pasquali, A. 2008, *PASP*, submitted
 Leitherer, C., et al. 1999, *ApJS*, 123, 3
 Madau, P., Haardt, F., & Rees, M. J. 1999, *ApJ*, 514, 648
 Madau, P., & Rees, M. J. 2000, *ApJ*, 542, L69
 Miralda-Escudé, J. 1998, *ApJ*, 501, 15
 Murdoch, H. S., Hunstead, R. W., Pettini, M., & Blades, J. C. 1986, *ApJ*, 309, 19
 Reimers, D., Fechner, C., Hagen, H.-J., Jakobsen, P., Tytler, D., & Kirkman, D. 2005, *A&A*, 442, 63
 Reimers, D., Köhler, S., Wisotzki, L., Groote, D., Rodríguez-Pascual, P., & Wamsteker, W. 1997, *A&A*, 327, 890
 Schneider, D. P., et al. 2005, *AJ*, 130, 367
 ———. 2007, *AJ*, 134, 102
 Spergel, D. N., et al. 2003, *ApJS*, 148, 175
 Stoughton, C., et al. 2002, *AJ*, 123, 485

- Theuns, T., Bernardi, M., Prieman, J., Hewett, P., Schaye, J., Sheth, R. K., & Subbarao, M. 2002, *ApJ*, 574, L111
- Tittley, E. R., & Meiksin, A. 2007, *MNRAS*, 380, 1369
- Walsh, J. R., Kümmel, M., & Larsen, S. S. 2006, in *Hubble after the Transition to Two-Gyro Mode*, ed. A. M. Koekemoer, P. Goudfrooij, & L. L. Dressel (Greenbelt: NASA/GSFC), 79
- Wolfe, A. M., Gawiser, E., & Prochaska, J. X. 2005, *ARA&A*, 43, 861
- Wyithe, J. S. B., & Loeb, A. 2003, *ApJ*, 586, 693
- Zheng, W., & Davidsen, A. F. 1995, *ApJ*, 440, L53
- Zheng, W., et al. 2004a, *AJ*, 127, 656
- . 2004b, *ApJ*, 605, 631
- . 2005, in *IAU Colloq. 199, Probing Galaxies through Quasar Absorption Lines*, ed. P. R. Williams, C. Shu, & B. Ménard (Cambridge: Cambridge Univ. Press), 484